


RESEARCH ARTICLE

Proportional loss of parvalbumin-immunoreactive synaptic boutons and granule cells from the hippocampus of sea lions with temporal lobe epilepsy

Starr Cameron¹ | Ariana Lopez^{1,2} | Raisa Glabman^{1,3} | Emily Abrams¹ | Shawn Johnson⁴ | Cara Field⁴ | Frances M. D. Gulland⁴ | Paul S. Buckmaster^{1,5} 

¹Department of Comparative Medicine, Stanford University, Stanford, California

²College of Veterinary Medicine, North Carolina State University, Raleigh, North Carolina

³School of Veterinary Medicine, University of Pennsylvania, Philadelphia, Pennsylvania

⁴The Marine Mammal Center, Sausalito, California

⁵Department of Neurology & Neurological Sciences, Stanford University, Stanford, California

Correspondence

Paul Buckmaster, Department of Comparative Medicine, Stanford University, 300 Pasteur Drive, Stanford, CA 94305.
Email: psb@stanford.edu

Present address

Starr Cameron, University of Wisconsin, Madison, WI
and

Raisa Glabman, Michigan State University, East Lansing, MI

Funding information

National Institute of Environmental Health Sciences, Grant/Award Number: R01 ES021960; National Institute of Neurological Disorders and Stroke, Grant/Award Number: R01 NS039110; National Science Foundation, Grant/Award Number: ES021960; NIH Office of the Director, Grant/Award Number: T35 OD010989

Abstract

One in 26 people develop epilepsy and in these temporal lobe epilepsy (TLE) is common. Many patients display a pattern of neuron loss called hippocampal sclerosis. Seizures usually start in the hippocampus but underlying mechanisms remain unclear. One possibility is insufficient inhibition of dentate granule cells. Normally parvalbumin-immunoreactive (PV) interneurons strongly inhibit granule cells. Humans with TLE display loss of PV interneurons in the dentate gyrus but questions persist. To address this, we evaluated PV interneuron and bouton numbers in California sea lions (*Zalophus californianus*) that naturally develop TLE after exposure to domoic acid, a neurotoxin that enters the marine food chain during harmful algal blooms. Sclerotic hippocampi were identified by the loss of Nissl-stained hilar neurons. Stereological methods were used to estimate the number of granule cells and PV interneurons per dentate gyrus. Sclerotic hippocampi contained fewer granule cells, fewer PV interneurons, and fewer PV synaptic boutons, and the ratio of granule cells to PV interneurons was higher than in controls. To test whether fewer boutons was attributable to loss versus reduced immunoreactivity, expression of synaptotagmin-2 (syt2) was evaluated. Syt2 is also expressed in boutons of PV interneurons. Sclerotic hippocampi displayed proportional losses of syt2-immunoreactive boutons, PV boutons, and granule cells. There was no significant difference in the average numbers of PV- or syt2-positive boutons per granule cell between control and sclerotic hippocampi. These findings do not address functionality of surviving synapses but suggest reduced granule cell inhibition in TLE is not attributable to anatomical loss of PV boutons.

KEYWORDS

dentate gyrus, granule cell, parvalbumin, RRID:AB_10000344, RRID:AB_10013783, sea lion, synaptic bouton, synaptotagmin-2, temporal lobe epilepsy

1 | INTRODUCTION

In human patients with temporal lobe epilepsy (TLE) seizures usually start in the hippocampus (Quesney, 1986; Spanedda, Cendes, & Gotman, 1997; Spencer, Williamson, Spencer, & Mattson, 1987; Sperling & O'Connor, 1989). The hippocampal dentate gyrus is suspected to play an epileptogenic role in part because it is hyperexcitable (Franck, Pokorny, Kunkel, & Schwartzkroin, 1995; Masukawa et al., 1995), it can generate seizure activity (Gabriel et al., 2004), and

dentate granule cells are less inhibited than in controls (Williamson, Patrylo, & Spencer, 1999; Williamson, Spencer, & Spencer, 1995). In three different rodent models of TLE, reduced inhibition of granule cells is evident as abnormally low frequencies of miniature inhibitory postsynaptic currents (Kobayashi & Buckmaster, 2003; Shao & Dudek, 2005; Sun, Mtchedlishvili, Bertram, Erisir, & Kapur, 2007). Most miniature inhibitory postsynaptic currents recorded in granule cells are generated by perisomatic synapses (Soltesz, Smetters, & Mody, 1995). Parvalbumin-positive basket cells are a major source of inhibitory

synaptic input to granule cell somata (Kraushaar & Jonas, 2000). Reduced inhibition of granule cells might be attributable to fewer synapses from parvalbumin-positive interneurons.

In human patients with TLE neuron loss is common in the hippocampus (Margerison & Corsellis, 1966). Tissue surgically resected to treat human patients displays fewer parvalbumin interneurons in the dentate gyrus compared to controls (Andrioli, Alonso-Nanclares, Arellano, & DeFelipe, 2007; Arellano, Muñoz, Ballesteros-Yáñez, Sola, & DeFelipe, 2004; Sloviter, Sollas, Barbaro, & Laxer, 1991; Zhu, Armstrong, Hamilton, & Grossman, 1997). However, many patients also display partial loss of granule cells (Babb, Pretorius, Kupfer, & Crandall, 1989; Bahh et al., 1999; Blümcke et al., 2007; de Lanerolle et al., 2003; Kim, Guimaraes, Shen, Masukawa, & Spencer, 1990; Mathern et al., 1996; Mathern, Babb, Pretorius, & Leite, 1995; Mathern, Kuhlman, Mendoza, & Pretorius, 1997; Sass et al., 1990). If granule cell and interneuron losses were proportional, normal levels of parvalbumin interneuron-mediated inhibition might be maintained.

Reductions in parvalbumin-immunoreactivity can occur without cell death (Bazzett, Becker, Falik, & Albin, 1994; Johansen, Tønder, Zimmer, Baimbridge, & Diemer, 1990; Kim et al., 2006; Scotti, Bollag, Kalt, & Nitsch, 1997; Tortosa & Ferrer, 1993). Wittner et al. (2001) reported fewer parvalbumin interneurons in the dentate gyrus of patients with TLE. At the electron microscopic level, however, inhibitory synaptic input to granule cell somata appeared relatively normal. Expression of synaptotagmin-2 might help distinguish between actual losses of synaptic boutons versus reduced immunodetection. Synaptotagmin-2 is an evolutionarily conserved Ca^{2+} sensor for exocytosis (Geppert, Archer 3rd, & Südhof, 1991; Südhof, 2013). Many parvalbumin-positive synaptic boutons are immunoreactive for synaptotagmin-2 (García-Junco-Clemente et al., 2010; Sommeijer & Levelt, 2012). It is not known whether the number of parvalbumin-positive and synaptotagmin-2-positive synaptic boutons per granule cell change with TLE.

Studies of human tissue provide direct insight into the pathology of TLE but can be limited by a lack of ideal control material and compromised tissue preservation. Surgical resections include only part of the hippocampus resulting in incomplete sampling. Those constraints do not pertain to rodent models of TLE, but rodent models do not replicate the extent of granule cell loss (Buckmaster & Lew, 2011; Mello et al., 1993; Thind et al., 2010; Yamawaki, Thind, & Buckmaster, 2015), and they rarely display parvalbumin cell loss as severe as in many human patients (André, Marescaux, Nehlig, & Fritschy, 2001; Buckmaster & Dudek, 1997; Huusko, Römer, Ndode-Ekane, Lukasiuk, & Pitkänen, 2015; Sun et al., 2007; but see van Vliet, Aronica, Tolner, Lopes da Silva, & Gorter, 2004).

This study evaluated a novel, large animal model that reproduces key aspects of human TLE pathology in the dentate gyrus. California sea lions (*Zalophus californianus*) are wild human-sized carnivores that live on the west coast of North America and are exposed to the glutamate receptor agonist domoic acid when it is produced by oceanic algae during seasonal blooms (Scholin et al., 2000). Naturally occurring domoic acid intoxication can cause status epilepticus, and many surviving sea lions develop epilepsy (Goldstein et al., 2008; Greig, Gulland, & Kreuder, 2005; Gulland et al., 2002; Montie et al., 2012; Thomas, Harvey, Goldstein, Barakos, & Gulland, 2010). The neuropathology of epileptic sea lions is similar to that of human patients with TLE, including unilateral hippocampal sclerosis in

most cases and partial loss of granule cells in sclerotic hippocampi (Buckmaster, Wen, Toyoda, Gulland, & Van Bonn, 2014; Silvagni, Lowenstine, Spraker, Lipscomb, & Gulland, 2005). To learn more about the potential role of parvalbumin interneuron synaptic input to granule cells in TLE, we asked whether epileptic sea lions have fewer parvalbumin-positive interneurons per dentate gyrus, fewer parvalbumin- and synaptotagmin-2-positive synaptic boutons per dentate gyrus, and fewer parvalbumin- and synaptotagmin-2-positive boutons per granule cell compared to controls.

2 | MATERIALS AND METHODS

2.1 | Animals

Subjects were California sea lions that stranded along the central California coast in 2010–2015 and were admitted to The Marine Mammal Center in Sausalito, California for rehabilitation but did not respond to treatment and were euthanized due to poor prognosis for release. Stranded sea lions were collected under a Letter of Authorization from the National Marine Fisheries Service to The Marine Mammal Center. Sex and age determination was based on established criteria (Greig et al., 2005): pup (0–1 years), yearling (1–2 years), juvenile male (2–4 years), subadult male (4–8 years), juvenile or subadult female (2–5 years), adult male (8+ years), and adult female (5+ years).

Control subjects (nine females, three males, and one unknown) were pups ($n = 1$), yearlings ($n = 1$), juveniles ($n = 1$), subadults ($n = 1$), or adults ($n = 8$) that were euthanized because of leptospirosis, septicemia, trauma, or gunshot wounds. Three of the control subjects were observed to have a spontaneous seizure; one had evidence of infectious encephalitis, but hippocampal neuron loss was not apparent in any of the control sea lions.

Sea lions that survive acute domoic acid toxicosis can develop epilepsy that is consistently associated with hippocampal atrophy (Goldstein et al., 2008). Hippocampal sclerosis in sea lions is most evident by hilar neuron loss (Buckmaster et al., 2014). Hippocampi were classified as sclerotic based on hilar neuron loss in Nissl-stained sections (Figure 1). Hilar neuron loss was evident bilaterally in 14 sea lions. Unilateral hippocampal sclerosis occurred in 17 sea lions (Figure 2). Unilateral hippocampal sclerosis was on the right side in 12 sea lions and on the left side in 5 sea lions. The proportion of right-sided unilateral sclerosis is not significantly greater than chance ($p > .05$; Daniel, 1987). Subjects with hippocampal sclerosis (18 females, 13 males) were juveniles ($n = 6$), subadults ($n = 10$), or adults ($n = 15$). The time between stranding (from the first stranding for those eight that restranded) and euthanasia was 43 ± 15 days (mean \pm SEM, range = 4–383 days, median = 18 days). While at The Marine Mammal Center, 21 subjects with hippocampal sclerosis (68%) were observed by chance to have at least one spontaneous seizure and nine of those had multiple seizures.

This study consists of four hippocampal groups: controls, bilateral sclerotics, unilateral sclerotics, and unilateral non-sclerotics. Unilateral non-sclerotics are a within animal control for unilateral sclerotic hippocampi.

Immediately after they were euthanized by intravenous pentobarbital overdose sea lions were perfused intracardially at 1 L/min for 2 min with 0.9% NaCl then 30 min with 4°C 4% formaldehyde in

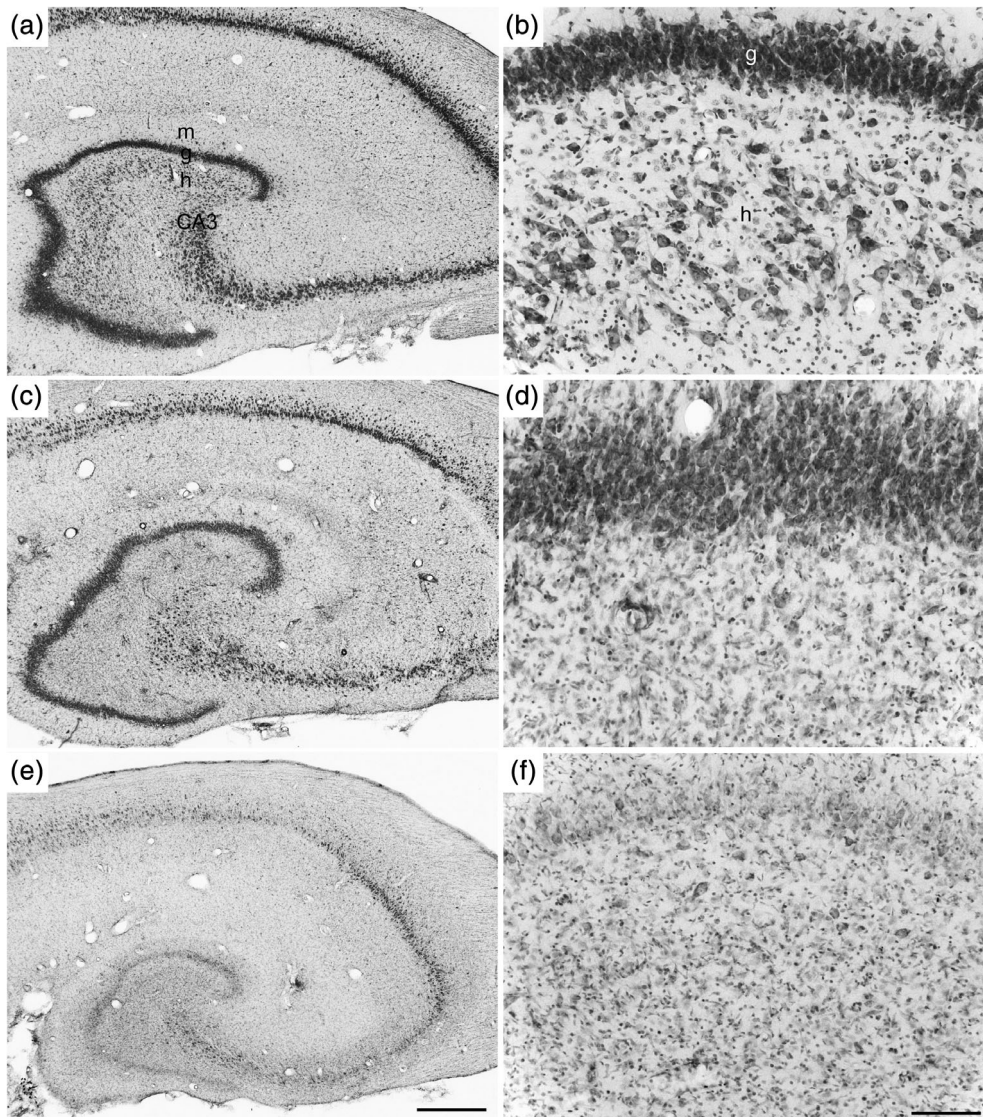


FIGURE 1 Sclerotic hippocampi were identified by hilar neuron loss in Nissl-stained sections. (Panels a, b) Control sea lion (adult female) with abundant neurons in the hilus (h). (Panels c, d) Sclerotic hippocampus from a juvenile male with hilar neuron loss but preservation of granule cells. (Panels e, f) Sclerotic hippocampus from an adult female with loss of hilar neurons and granule cells. Scale bar in panel e = 400 μm and applies to panels a, c. Scale bar in panel f = 50 μm and applies to panels b, d. Abbreviations: g: granule cell layer; m: molecular layer; CA3: proximal tip of the CA3 pyramidal cell layer

0.1 M phosphate buffer (PB, pH 7.4). Brains were hemisected and then cut coronally into ~ 2 cm thick blocks. The middle block was bordered rostrally by the anterior tip of the temporal lobe, and it contained the entire hippocampus in most animals. In some sea lions, the next caudal block also contained part of the hippocampus, and it was also evaluated. Blocks postfixed in 4°C 4% formaldehyde and 30% sucrose in 0.1 M PB until equilibrating, which took ~ 1 week. Blocks were then frozen in isopentane and stored at -80°C .

2.2 | Section sampling

Blocks were sectioned coronally at 40 μm using a sliding microtome equipped with a freezing stage. Sections were collected in 30% ethylene glycol and 25% glycerol in 50 mM PB and stored at -20°C . Starting at a random section near the tip of the temporal lobe, a 1-in-40 series of sections was Nissl-stained with 0.25% thionin. Adjacent

1-in-40 series of sections were processed for parvalbumin- or synaptotagmin-2-immunocytochemistry.

2.3 | Staining

After rinses in PB, free-floating sections were exposed to 1% hydrogen peroxide in PB for 2 hr. Following rinses in 0.1 M tris-buffered saline (TBS, pH 7.4), sections were exposed to blocking solution consisting of 3% goat serum, 2% bovine serum albumin (BSA), and 0.3% triton X-100 in TBS for 1 hr. After rinses in TBS, sections were incubated for 7 days at 4°C in antiserum (Table 1) diluted in 1% goat serum and 0.2% BSA in TBS. After rinsing in TBS, sections were exposed for 2 hr to biotinylated anti-rabbit or anti-mouse serum (1:500, Vector Laboratories, Burlingame, California) in secondary diluent consisting of 2% BSA and 0.3% triton X-100 in TBS. After rinsing in TBS, sections were exposed to avidin-biotin-horse radish

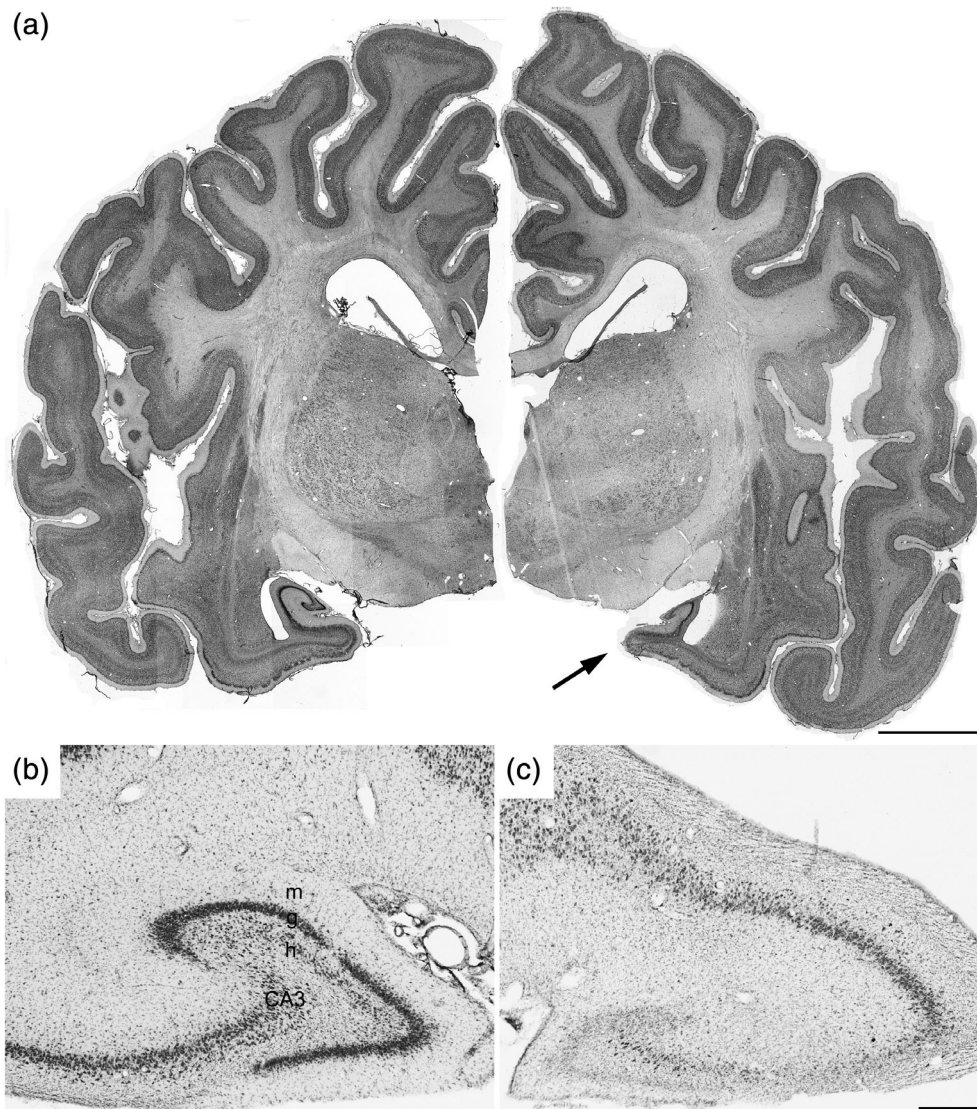


FIGURE 2 Nissl-stained coronal sections of cerebral hemispheres reveal unilateral hippocampal sclerosis in an adult female sea lion (panel a). The right hippocampus (arrow) is sclerotic and smaller than the left hippocampus. Scale bar = 1 cm. Higher magnification of the left (panel b) and right hippocampus (panel c) reveals substantial loss of pyramidal cells, hilar neurons, and granule cells in the right hippocampus. Scale bar = 500 μ m. Abbreviations: h: hilus; g: granule cell layer; m: molecular layer; CA3: proximal tip of CA3 pyramidal cell layer

peroxidase complex (1:500, Vector Laboratories) in secondary diluent for 2 hr. After rinses in TBS, sections were exposed to 0.02% diaminobenzidine, 0.04% ammonium chloride, 0.015% glucose oxidase, and 0.1% β -D-glucose in 0.1 M tris buffer (TB, pH 7.4) for 13 min. After rinses in TB, sections were mounted on slides and cover slipped with distyrene plasticizer xylene.

2.4 | Antibody characterization

Primary antibodies are described in Table 1. According to the manufacturer's data sheet, the parvalbumin antibody does not stain cells in the brain of parvalbumin knockout mice. In the sea lion hippocampus, the

antibody stained a pattern consistent with parvalbumin-positive neurons demonstrated previously in other species (Kosaka, Katsumaru, Hama, Wu, & Heizmann, 1987).

The synaptotagmin-2 antibody was identified in a screen of zebrafish tissue (Trevarrow, Marks, & Kimmel, 1990). Mass spectrometry was used to identify synaptotagmin-2 as the protein immunoprecipitated by this antibody (Fox & Sanes, 2007). The antibody detects a single band at 60 kDa in Western blots of mouse cerebellum, hippocampus, and synaptosomal fractions but not liver. In the sea lion hippocampus, the antibody stained a pattern consistent with synaptotagmin-2-positive boutons in mice (Fox & Sanes, 2007; García-Junco-Clemente et al., 2010).

TABLE 1 Primary antibodies used in this study

Antibody	Immunogen	Source	Concentration
Parvalbumin	Rat muscle parvalbumin	Swant, PV 25, rabbit polyclonal, RRID: AB_10000344	1:5,000
Synaptotagmin-2	Homogenized zebrafish embryo	Zebrafish International Research Center, znp-1, mouse monoclonal, RRID: AB_10013783	1:1,000

2.5 | Analysis

The optical fractionator method (West, Slomianka, & Gundersen, 1991) was used to evaluate a 1-in-40 series, which was an average of 10 sections with dentate gyrus per hippocampus for each stain. To estimate numbers of granule cells, a 10 \times objective was used to outline the Nissl-stained granule cell layer, which was sampled using Stereo Investigator (MBF Bioscience, Williston, Vermont). The counting frame was 10 \times 10 μm , and the counting grid was 150 \times 150 μm . Dissector height was total section thickness. Nuclei not cut at the superficial surface were counted using a 100 \times objective and a Lucivid (MBF Bioscience). An average of 152 granule cells per hippocampus was counted. The mean coefficient of error (0.144) was only one-fifth of the coefficient of variation (0.717) suggesting only a small part of the group variance was attributable to the within animal estimation procedure.

To estimate the number of parvalbumin-positive somata, the entire dentate gyrus in each section was examined with a 20 \times objective, and an average of 215 parvalbumin-positive cell body profiles per hippocampus was counted (NeuroLucida; MBF Bioscience). An established method was used to estimate neuron numbers per dentate gyrus from profile counts (Buckmaster, Abrams, & Wen, 2017). A subset of five hippocampi with a range of profile counts (17–680) was analyzed further using the optical fractionator method to measure the number of parvalbumin-positive neurons per dentate gyrus. All profiles were examined with a 100 \times objective and only those not cut at the superficial surface of the section were counted. From a plot of profiles versus neurons per dentate gyrus, a regression line was calculated ($r = 0.999$) and its slope was used to convert profile counts to neurons per hippocampus for all samples.

To estimate the number of parvalbumin- and synaptotagmin-2-positive boutons, a 10 \times objective was used to outline the cloud of boutons associated with the granule cell layer. Then a 100 \times objective was used to count boutons in a sampled subregion (Stereo Investigator, MBF Biosciences). The counting frame was 5 \times 5 μm and the counting grid was 300 \times 300 μm . Axonal swellings were counted if they were not cut at the superficial surface of the section and were at least ~ 1 μm in diameter. Boutons making basket cell-to-granule cell synapses are larger in epileptic pilocarpine-treated rats compared to controls (Buckmaster, Yamawaki, & Thind, 2016), so although unlikely, it is possible that larger boutons might have resulted in relatively higher counts in epileptic animals. An average of 155 parvalbumin-immunoreactive (PV) boutons was counted per hippocampus. The mean coefficient of error (0.12) was much less than the coefficient of variation (0.73). For synaptotagmin-2-immunoreactive boutons, an average of 131 boutons was counted per hippocampus, and the mean coefficient of error (0.17) was much less than the coefficient of variation (0.97).

2.6 | Statistics

SigmaPlot 12 (Systat Software) was used for statistical analyses.

2.7 | Images

Photoshop version 12.0 (Adobe) was used to process images. Only brightness and contrast were adjusted.

3 | RESULTS

3.1 | Parvalbumin-immunoreactivity

In the dentate gyrus of control sea lions and in nonsclerotic hippocampi of epileptic sea lions, PV axons and boutons formed a continuous dense meshwork in the granule cell layer (Figures 3a, 4a, and 5a,b). PV axons and boutons also were concentrated in the pyramidal cell layers of the hippocampal formation. Parvalbumin-positive somata in the dentate gyrus were found in the molecular layer, granule cell layer, and hilus, and were most abundant near the border of the granule cell layer and hilus. Soma shapes were mainly multipolar and sometimes fusiform (Figures 3a and 5a–c). Dendrites were mostly aspiny, sometimes beaded, and they extended through the molecular layer and hilus. These findings are similar to reports of parvalbumin-immunoreactivity in other species, including mice (Jinno & Kosaka, 2002), gerbils (Nitsch, Scotti, & Nitsch, 1995; Seto-Ohshima, Aoki, Semba, Emson, & Heizmann, 1990), rats (Celio, 1986; Kosaka et al., 1987), mole-rats (Amrein et al., 2014), guinea pigs (Nacher, Palop, Ramirez, Molowny, & Lopez-Garcia, 2000), hedgehogs (Ferrer, Zujar, Admella, & Alcantara, 1992), rabbits (de Jong et al., 1996), tree shrews (Keuker, Rochford, Witter, & Fuchs, 2003), elephant shrews (Slomianka et al., 2013), pigs (Holm, Geneser, Zimmer, & Baimbridge, 1990), cats (Mitchell, Buckmaster, Hoover, Whalen, & Dudek, 1999), dogs (Hof, Rosenthal, & Fiskum, 1996), foxes (Amrein & Slomianka, 2010), monkeys (Austin & Buckmaster, 2004; Pitkänen & Amaral, 1993; Seress, Gulyás, & Freund, 1991), and humans (Braak, Strotkamp, & Braak, 1991; Seress et al., 1993).

In sclerotic hippocampi, the number of PV somata, dendrites, axons, and boutons appeared to be reduced to variable degrees especially in the dentate gyrus (Figures 3b, 4b,c, and 5c–f). The reduced immunoreactivity did not appear to be attributable to problems with the staining procedure, because some well-labeled neurons, dendrites, and axons persisted in all tissue sections. Even in sections where many fewer parvalbumin-positive somata, dendrites, axons, and boutons were evident, those still visible were well labeled. In some parts of the granule cell layer, parvalbumin-immunoreactivity appeared to be absent. In some of those cases, examination of adjacent Nissl-stained sections revealed very few surviving granule cells. In other cases, however, granule cells were evident in regions devoid of parvalbumin-positive axons and boutons (Figure 4b,h).

3.2 | Quantitative analysis

3.2.1 | Granule cells

Nissl staining clearly revealed the granule cell layer (Figures 2b, 4g–i). The average number of granule cells per hippocampus in control sea lions was 2,320,000 (Table 2 and Figure 6a), similar to that reported previously (Buckmaster et al., 2014). The value plotted for each control (and bilateral sclerotic) sea lion is the average of the right and left hippocampus from that individual. In sea lions with bilateral sclerosis, the average number of granule cells was only 22% of controls ($p < .05$, Kruskal–Wallis ANOVA on ranks with Dunn's method). In sea lions with unilateral sclerosis, results are divided into sclerotic and nonsclerotic hippocampal groups. The average number of granule cells

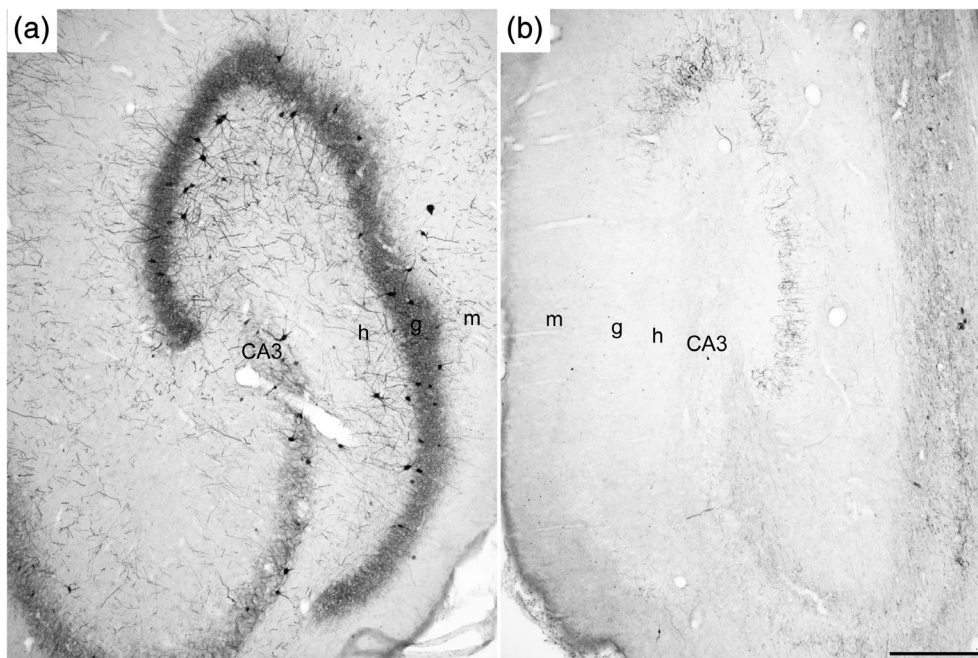


FIGURE 3 Parvalbumin-immunoreactivity in the left (a) and right (b) dentate gyrus of an adult female sea lion with right unilateral hippocampal sclerosis. Cell layers indicated. Scale bar = 500 μ m. Abbreviations: h: hilus; g: granule cell layer; m: molecular layer; CA3: proximal tip of CA3 pyramidal cell layer

in nonsclerotic hippocampi was similar to controls. The average number of granule cells in sclerotic hippocampi was reduced to only 31% of controls ($p < .05$). The number of granule cells in unilaterally sclerotic hippocampi was 1.4-times that of bilateral sclerotic hippocampi but not significantly different. These findings confirm partial loss of granule cells in sea lions with hippocampal sclerosis.

3.2.2 | PV neurons

Control sea lions had 10,700 parvalbumin-positive neurons per dentate gyrus (Table 2 and Figure 6b). In sea lions with bilateral sclerosis, the average number of parvalbumin neurons per dentate gyrus was only 5% of controls ($p < .05$). The average number of parvalbumin neurons in nonsclerotic hippocampi was similar to controls. The average number of parvalbumin neurons in unilaterally sclerotic hippocampi was only 4% of controls ($p < .05$) and similar to that of bilateral sclerotic hippocampi. These findings reveal severe loss of PV neurons in the dentate gyrus of sea lions with hippocampal sclerosis.

The ratio of granule cells to parvalbumin-positive neurons was calculated for each hippocampus. Control sea lions had 227 ± 15 granule cells per parvalbumin-positive neuron (median = 221; Figure 6c). In sea lions with bilateral sclerosis, the average number of granule cells per parvalbumin-positive neuron was 11-times that of controls ($2,510 \pm 1,050$; median = 1,230; $p < .05$). The average number of granule cells per parvalbumin-positive neuron in nonsclerotic hippocampi was similar to controls (226 ± 17 ; median = 219). The average number of granule cells per parvalbumin-positive neuron in sclerotic hippocampi ($3,260 \pm 1,530$; median = 1,420) was 14-times that of controls ($p < .05$) and not significantly different than that of bilateral sclerotic hippocampi. These findings reveal relatively fewer PV interneurons compared to granule cells in sclerotic hippocampi.

3.2.3 | PV boutons

Inhibition of granule cells might be more directly related to the number of parvalbumin-positive synaptic boutons than the number of somata. Control sea lions had an average of 37.6 million granule cell layer-associated PV boutons per dentate gyrus (Table 2 and Figure 6d). In sea lions with bilateral sclerosis, the average number of parvalbumin-positive boutons was only 27% of controls. The average number of parvalbumin-positive boutons in nonsclerotic hippocampi was similar to controls. The average number of parvalbumin-positive boutons in unilaterally sclerotic hippocampi was only 29% of controls ($p < .05$) and similar to that of bilateral sclerotic hippocampi. These findings reveal loss of PV boutons in the dentate gyrus of sclerotic hippocampi.

The number of PV boutons per parvalbumin-positive interneuron was calculated for each hippocampus. Control sea lions had $3,700 \pm 300$ parvalbumin-positive boutons per interneuron (median = 3,400; Figure 6e). In sea lions with bilateral sclerosis, the average number of parvalbumin-positive boutons per interneuron was over 11-times that of controls ($42,900 \pm 8,800$; median = 42,200; $p < .05$). The average number of parvalbumin-positive boutons per interneuron in nonsclerotic hippocampi was similar to controls ($3,400 \pm 300$; median = 3,300). The average number of parvalbumin-positive boutons per interneuron in sclerotic hippocampi ($47,100 \pm 16,600$; median = 22,300) was over 12-times that of controls ($p < .05$) and similar to that of bilateral sclerotic hippocampi. These findings reveal increased ratios of parvalbumin-positive boutons per interneuron in sclerotic hippocampi.

To test whether synaptic input from parvalbumin interneurons to individual granule cells might be different in sclerotic versus control hippocampi, the average number of parvalbumin-positive boutons per granule cell was calculated for each hippocampus. This calculation assumes that all parvalbumin-positive boutons synapse only with granule cells, which is not strictly true. For example, PV boutons also synapse with

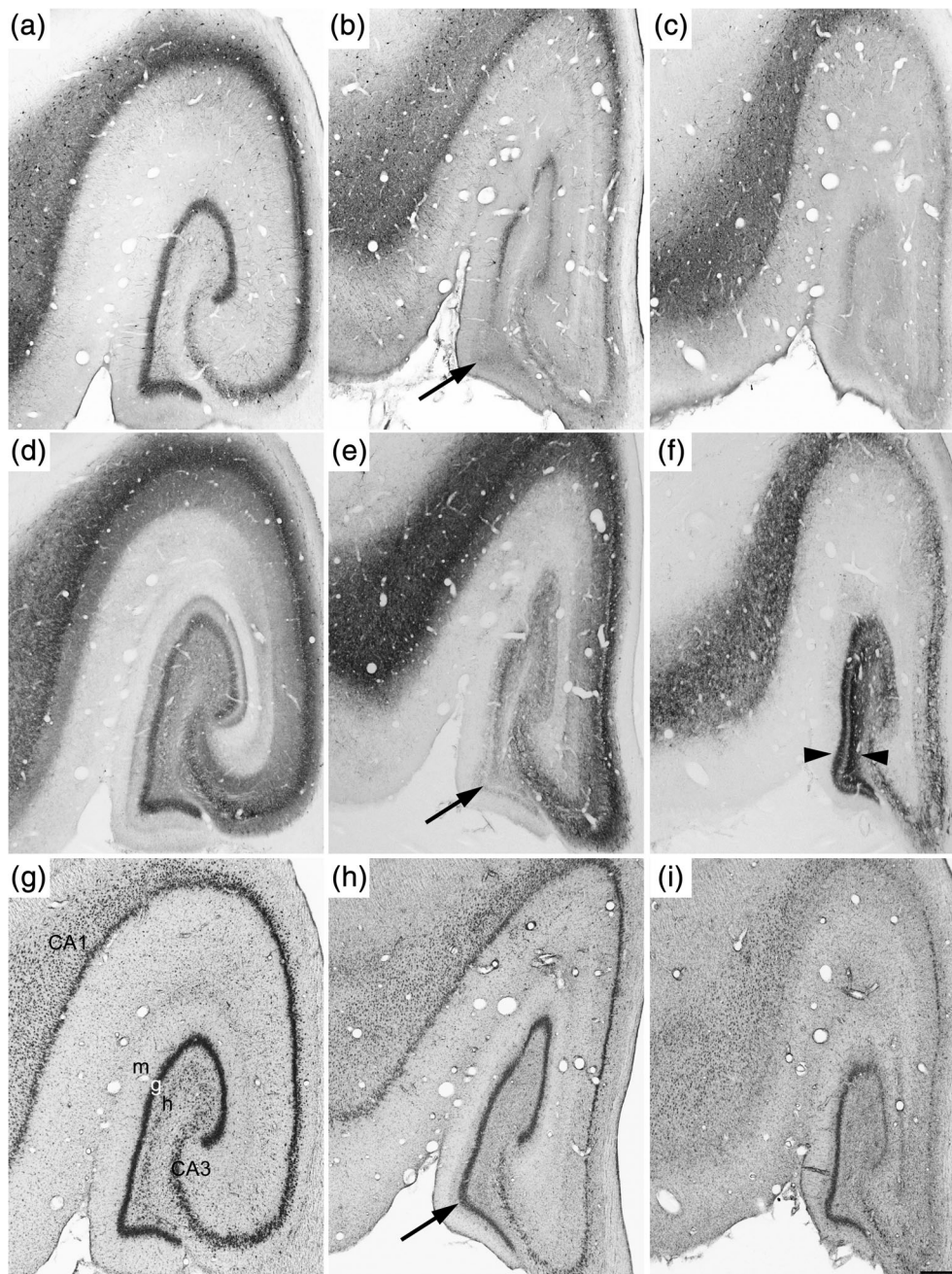


FIGURE 4 Parvalbumin-immunoreactivity (panels a–c), synaptotagmin-2-immunoreactivity (panels d–f), and Nissl staining (panels g–i) of hippocampi from an adult female control sea lion (panels a, d, g), a juvenile male sea lion with bilateral sclerosis (panels b, e, h), and an adult male sea lion with bilateral sclerosis (panels c, f, i). (g) Cell layers indicated. In one of the sea lions with bilaterally sclerotic hippocampi, arrows indicate part of the granule cell layer containing granule cells (panel h) but devoid of parvalbumin- (panel b) and synaptotagmin-2-immunoreactive boutons (panel e). (Panel f) In another sea lion with bilaterally sclerotic hippocampi, arrowheads indicate aberrant synaptotagmin-2-immunoreactivity in the inner molecular layer and hilus. Scale bar = 500 μ m. Abbreviations: h: hilus; g: granule cell layer; m: molecular layer; CA3: proximal tip of the CA3 pyramidal cell layer

parvalbumin-positive interneurons (Fukuda, Aika, Heizmann, & Kosaka, 1996). Our calculations might overestimate the parvalbumin innervation of granule cells, but probably only to a minor extent. Control sea lions had 16.7 ± 1.2 parvalbumin-positive boutons per granule cell (median = 16.1; Figure 6f). In sea lions with bilateral sclerosis, the average number of parvalbumin-positive boutons per granule cell (41.9 ± 13.0) was 2.5-times that of controls, and the median (26.2) was 1.6-times that of controls, but the difference was not statistically significant. The average number of parvalbumin-positive boutons per granule cell in nonsclerotic hippocampi was similar to controls (15.8 ± 1.4 ; median = 15.8). The average number

of parvalbumin-positive boutons per granule cell in sclerotic hippocampi was 23.3 ± 4.6 (median = 15.9). The differences in median values among all the hippocampal groups were not statistically significant ($p = .452$).

3.3 | Synaptotagmin-2-immunoreactivity

Parvalbumin in surviving cells can become undetectable by immunocytochemical methods after various conditions including seizure activity (see Section 1). Thus, it is possible that interneuron somata and boutons that once expressed parvalbumin survived in epileptic sea lions but lost their

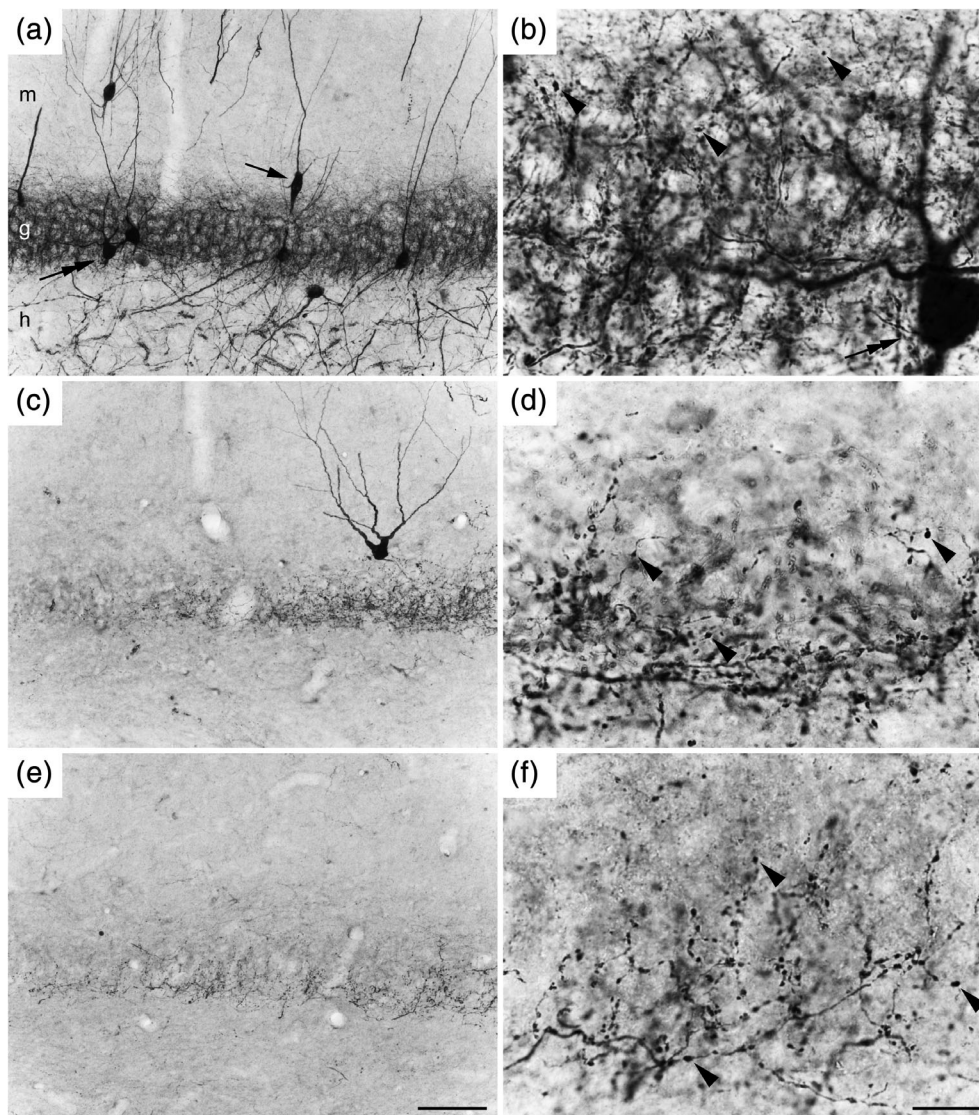


FIGURE 5 Higher magnification views of parvalbumin-immunoreactivity in the dentate gyrus of the same control sea lion (panels a, b) and same two sea lions with bilateral sclerosis (panels c–f) shown at lower magnification in Figure 4. A fusiform (arrow) and a multipolar (double arrow) soma are indicated (panels a, b). Some boutons are indicated by arrowheads (panels b, d, f). Scale bar in panel e = 100 μ m and applies to panels a, c. Scale bar in panel f = 20 μ m and applies to panels b, d. Abbreviations: h: hilus; g: granule cell layer; m: molecular layer

immunoreactivity. We used synaptotagmin-2-immunoreactivity to test whether changes in parvalbumin-positive synaptic boutons in sclerotic hippocampus might be attributable to marker dropout. Synaptotagmin-2-immunoreactivity might persist in surviving boutons that stop expressing parvalbumin. For example, rearing mice under dark conditions reduces expression of parvalbumin in synaptic boutons in the visual cortex, but synaptotagmin-2 expression continues (Fox & Sanes, 2007). Seizure activity does not affect the expression of synaptotagmin-2 in the hippocampus (Elfving, Bonefeld, Rosenberg, & Wegener, 2008). The cellular pattern of expression of synaptotagmin-2 mRNA in the dentate gyrus is consistent with that of parvalbumin interneurons (Marquèze et al., 1995; Pang et al., 2006). In the control mouse, visual cortex synaptotagmin-2 is expressed in almost all parvalbumin-positive boutons and vice versa (Sommeijer & Levelt, 2012). In the mouse granule cell layer, levels of coexpression of synaptotagmin-2 and parvalbumin are high (García-Junco-Clemente et al., 2010).

In control sea lions, synaptotagmin-2-immunoreactivity was evident in the hippocampal formation including the dentate gyrus (Figures 4d and 7a,b). In the inner molecular layer there was light background staining. In the hilus, there was light background staining and darkly labeled synaptotagmin-2-positive boutons. The granule cell layer contained the highest density of synaptotagmin-2-positive boutons. Synaptotagmin-2 appeared to be expressed in synaptic boutons and not much in axon segments. Synaptotagmin-2-immunoreactivity was not evident in somata or dendrites. These findings are similar to previous reports for mouse hippocampus (Fox & Sanes, 2007), including the dentate gyrus (García-Junco-Clemente et al., 2010).

Synaptotagmin-2-immunoreactivity was reduced in most sclerotic hippocampi, especially in the dentate gyrus (Figures 4e and 7c,d). Reduced synaptotagmin-2-immunoreactivity did not appear to be a problem with the staining procedure because some darkly labeled synaptotagmin-2-positive boutons persisted in all tissue sections. Reduced synaptotagmin-

TABLE 2 Number of granule cells, parvalbumin-immunoreactive neurons, parvalbumin-immunoreactive synaptic boutons, and synaptotagmin-2-immunoreactive boutons per dentate gyrus in control sea lions and sea lions with bilateral or unilateral hippocampal sclerosis

	Control	Bilateral sclerotic	Unilateral nonsclerotic	Unilateral sclerotic
Sea lions	13	14	17	17
Hippocampi	26	28	17	17
<i>Granule cells (million)</i>				
Average	2.318	0.506 ^a	2.335	0.733 ^a
Median	2.281	0.435	2.461	0.729
SEM	0.083	0.101	0.110	0.144
<i>Parvalbumin neurons</i>				
Average	10,700	483 ^a	11,000	442 ^a
Median	10,600	369	11,800	309
SEM	600	111	800	93
<i>Parvalbumin boutons (million)</i>				
Average	37.6	10.0 ^a	37.0	10.8 ^a
Median	35.3	9.4	34.6	9.4
SEM	2.0	1.4	3.9	2.1
<i>Synaptotagmin-2 boutons (million)</i>				
Average	34.8	5.0 ^a	28.4	12.4 ^a
Median	35.0	4.4	26.5	3.6
SEM	2.8	0.9	2.7	6.4

^aLess than control, $p < .05$, Kruskal–Wallis ANOVA on ranks with Dunn's method.

2-immunoreactivity was most evident in the granule cell layer. Reduced staining appeared to be attributable to fewer boutons not to reduced expression in positive boutons. In some parts of the granule cell layer, synaptotagmin-2-immunoreactivity appeared to be absent. In some of those cases, adjacent Nissl-stained sections revealed few if any surviving granule cells. In other cases, granule cells were evident (Figure 4e,h).

In most sclerotic hippocampi, synaptotagmin-2-immunoreactivity was reduced in the hilus (Figure 4e). However, in 3 of 17 unilaterally sclerotic hippocampi and in 4 of 28 hippocampi from bilaterally sclerotic sea lions, the number of synaptotagmin-2-immunoreactive boutons in the granule cell layer appeared to be reduced, but dense staining occurred in the bordering regions of the hilus of inner molecular layer (Figures 4f and 7e,f). The source of the dense staining in the hilus and molecular layer is unclear.

The number of synaptotagmin-2-positive boutons in the granule cell layer was quantified. Control sea lions had an average of 34.8 million in the granule cell layer per dentate gyrus (Table 2 and Figure 8a). In sea lions with bilateral sclerosis, the average number of synaptotagmin-2-positive boutons was only 13% of controls ($p < .05$). The average number of synaptotagmin-2-positive boutons in non-sclerotic hippocampi was not significantly different than controls. The average number of synaptotagmin-2-positive boutons in sclerotic hippocampi was 36% of controls ($p < .05$) and not significantly different from bilateral sclerotic hippocampi. These findings reveal loss of

synaptotagmin-2-immunoreactive boutons in the dentate gyrus of sclerotic hippocampi.

The ratio of synaptotagmin-2- and parvalbumin-positive boutons per dentate gyrus was calculated for each animal (Figure 8b). Control sea lions had an average ratio of 0.94 ± 0.06 synaptotagmin-2- versus parvalbumin-positive boutons in the granule cell layer (median = 0.97). In sea lions with bilateral sclerosis, the average ratio was 0.61 ± 0.09 (median = 0.67). In sea lions with unilateral sclerosis, the average ratio (including both sclerotic and nonsclerotic hippocampi) was 1.00 ± 0.26 (median = 0.77). There was no significant difference among groups ($p = 0.057$). These findings reveal average ratios of synaptotagmin-2- versus parvalbumin-positive boutons close to one, although variability was evident especially in sclerotic hippocampi.

To test whether synaptic input from synaptotagmin-2-positive boutons to individual granule cells might be different in sclerotic versus control hippocampi, the average number of boutons per granule cell was calculated for each hippocampus. Control sea lions had 15.1 ± 1.2 synaptotagmin-2-positive boutons per granule cell (median = 14.4; Figure 8c) which was similar to that of sea lions with bilateral sclerosis (17.9 ± 5.1 ; median = 9.6), nonsclerotic hippocampi (12.3 ± 1.1 ; median = 11.1), and sclerotic hippocampi (17.4 ± 4.9 ; median = 11.5). There was no significant difference across groups in the number of synaptotagmin-2-positive boutons per granule cell ($p = .511$).

4 | DISCUSSION

The principal finding of this study is that sea lions with naturally occurring TLE exhibit loss of PV interneurons and synaptic boutons. The loss of parvalbumin-positive boutons is proportional to the loss of granule cells, and there is no significant difference in the average number of PV boutons per granule cell in control versus sclerotic hippocampi. The number of parvalbumin-positive boutons per granule cell has not been measured previously, but these results from sea lions suggest there might also be proportional losses of PV boutons and granule cells in human patients with TLE.

4.1 | Reduced numbers of PV somata

Control sea lions had an average of one parvalbumin-positive interneuron per 227 granule cells: a high ratio of parvalbumin interneurons versus granule cells compared to other species. In macaque monkeys, there are 28 granule cells per glutamic acid decarboxylase-positive neuron in the dentate gyrus, and 9% of glutamic acid decarboxylase-positive neurons are parvalbumin-positive (Austin & Buckmaster, 2004). Thus, there are 311 granule cells per parvalbumin-positive neuron in monkeys. Rats have an average of 1.1 million granule cells (Thind et al., 2010) and 2,944 parvalbumin-positive interneurons per dentate gyrus (Buckmaster & Dudek, 1997), yielding 374 granule cells per parvalbumin-positive interneuron. Mice have an average of 450,000 granule cells (Buckmaster & Lew, 2011; Yamawaki et al., 2015) and 950 parvalbumin-positive interneurons per dentate gyrus (Buckmaster et al., 2017), yielding 474 granule cells per parvalbumin-positive interneuron. The high ratio of parvalbumin-positive interneurons to granule

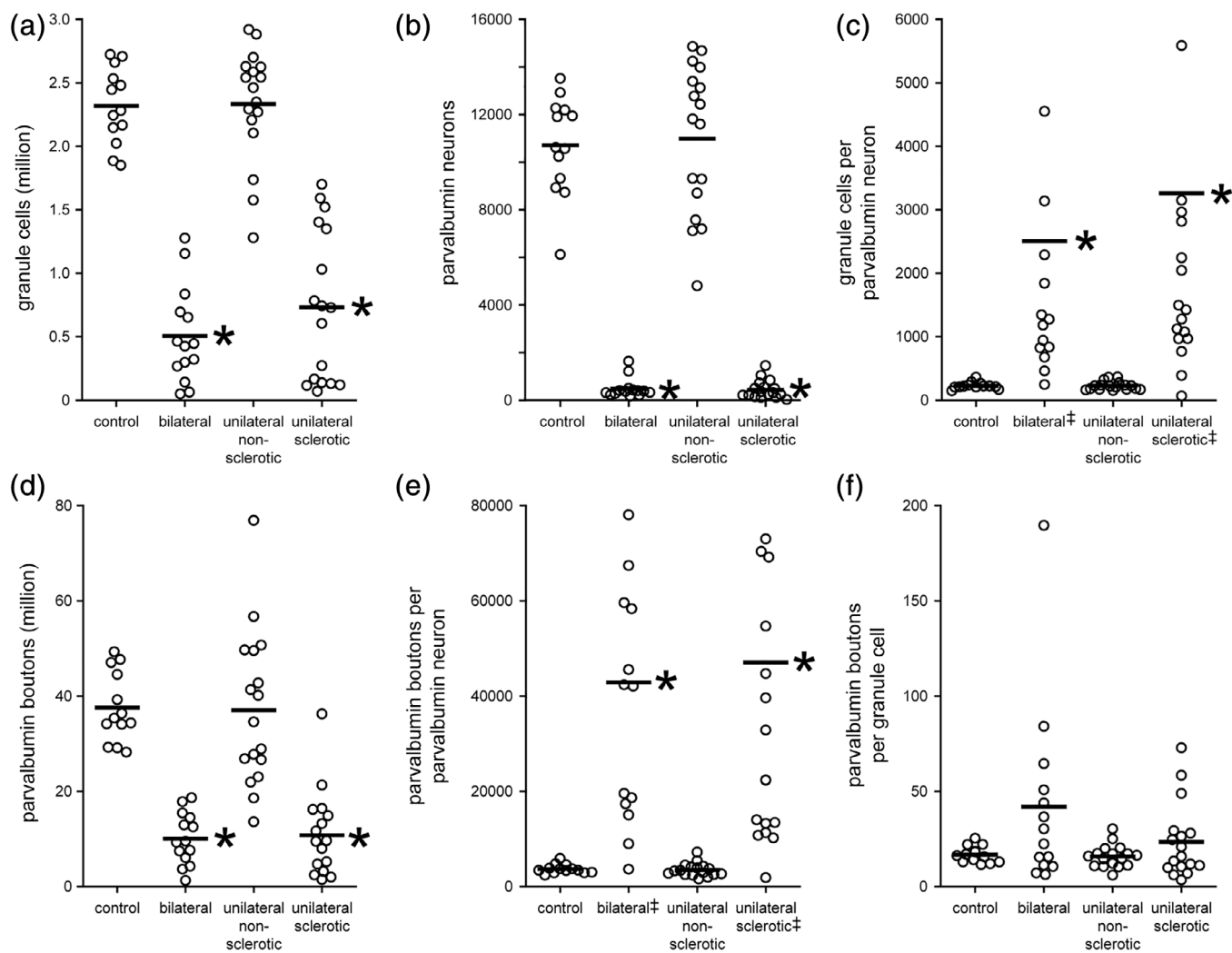


FIGURE 6 Number of granule cells (panel a), parvalbumin-immunoreactive neurons (panel b), granule cells per parvalbumin neuron (panel c), parvalbumin-immunoreactive boutons (panel d), parvalbumin boutons per parvalbumin neuron (panel e), and parvalbumin boutons per granule cell (panel f) in the dentate gyrus of control sea lions, sea lions with bilaterally sclerotic hippocampi, and sea lions with unilaterally sclerotic hippocampi (divided into nonsclerotic and sclerotic groups). Markers indicate values from individual sea lions. Bars indicate averages. Asterisks indicate significantly different from the control group, $p < .05$, Kruskal-Wallis ANOVA on ranks with Dunn's method. †Indicates groups in which one outlier value (≥ 2.5 -times the standard deviation from the average) is higher than the y axis scale of the plot

cells in sea lions might be related to their unusually low number of granule cells compared to other dentate gyrus neurons (Buckmaster et al., 2014).

The average number of PV neurons in the dentate gyrus of sclerotic hippocampi in sea lions was reduced to only 4–5% of controls. That reduction is much more severe than in rodent models of TLE (André et al., 2001; Buckmaster & Dudek, 1997; Huusko et al., 2015; Sun et al., 2007; van Vliet et al., 2004) and slightly more severe than in human patients (Andrioli et al., 2007; Wittner et al., 2001; Zhu et al., 1997). The extent to which reductions in parvalbumin-positive interneuron numbers are attributable to cell death versus marker dropout is unclear. Reduced parvalbumin staining can occur without interneuron death (see Section 1). If reductions were entirely due to cell death, then each surviving parvalbumin-positive interneuron would have an average of 11–14-times more granule cells to inhibit compared to control sea lions. Conversely, if reductions were entirely attributable to marker dropout, sclerotic hippocampi would have a 3.7-times relative excess of parvalbumin-positive interneurons versus

granule cells compared to control hippocampi. There might be some combination of PV cell death and marker dropout in sclerotic hippocampi. It remains unclear whether or not parvalbumin interneuron death is proportional to granule cell death in TLE.

4.2 | Reduced numbers of PV synaptic boutons

Control sea lions had an average of 3,700 parvalbumin-positive boutons per interneuron. This value is only 31–40% of that of biocytin-labeled parvalbumin-positive basket cells in CA1 of rats (Sik, Penttonen, Ylinen, & Buzsáki, 1995). It is not clear whether the difference is attributable to labeling technique, bouton counting criteria, hippocampal region, or species. It might be related to the low number of granule cells in sea lions compared to other neuron types in the dentate gyrus (Buckmaster et al., 2014), as fewer inhibitory synapses might be needed if there were fewer granule cells per interneuron.

Control sea lions had an average of 17 parvalbumin-positive boutons per granule cell. Rat granule cells reconstructed from serial

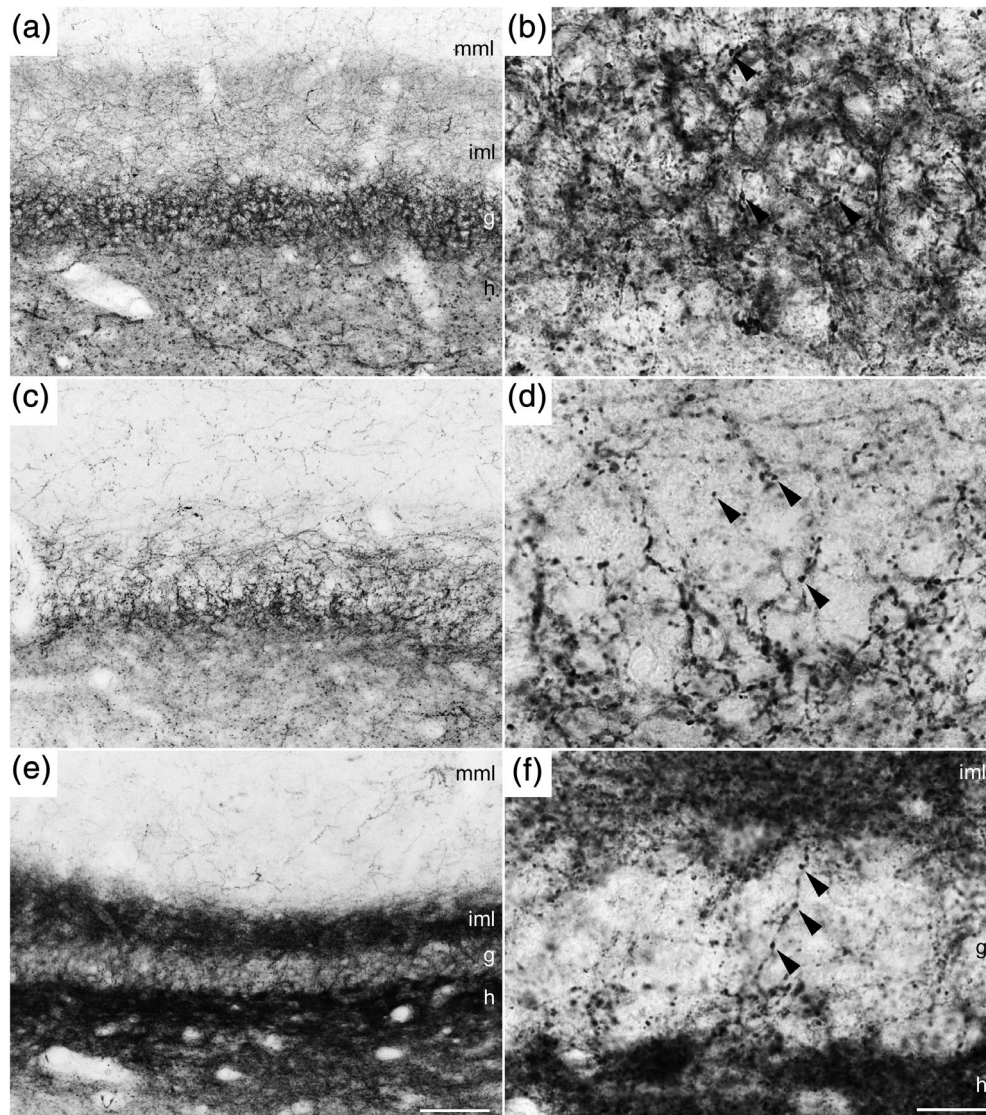


FIGURE 7 Higher magnification views of synaptotagmin-2-immunoreactivity in the dentate gyrus of the same control sea lion (panels a, b) and same two sea lions with bilateral sclerosis (panels c–f) shown at lower magnification in Figure 4. Some boutons are indicated by arrowheads (panels b, d, f). Scale bar in panel e = 100 μ m and applies to panels a, c. Scale bar in panel f = 20 μ m and applies to panels b, d. Abbreviations: h: hilus; g: granule cell layer; iml: inner molecular layer; mml: middle molecular layer

electron micrographs have an average of 52–69 symmetrical synapses on their soma and axon initial segment (Kosaka, 1996), and 38% are PV (Ribak, Nitsch, & Seress, 1990), yielding 20–26 parvalbumin-positive synapses per granule cell, a value close to that of control sea lions. Another study used electron microscopy and stereology to estimate that granule cells in rats have an average of 200 symmetrical synapses on their soma and axon initial segment (Thind et al., 2010). If 38% are PV (Ribak et al., 1990), then a rat granule cell would receive an average of 76 parvalbumin-positive synapses. At 17 parvalbumin-positive synapses per granule cell, control sea lions would have only 22% of that in rats. Sea lions, like monkeys, have much larger brains than rats, and monkeys have only 25% the number of axosomatic synapses per granule cell compared to rats (Seress & Ribak, 1992).

The average number of PV boutons associated with the granule cell layer was reduced to 27–29% of controls in sclerotic hippocampi of sea lions. To test whether the reduction was attributable to marker dropout,

a second marker was used. The average number of synaptotagmin-2-immunoreactive boutons associated with the granule cell layer in sclerotic hippocampi of sea lions was reduced to 13–36% of controls, which is more variable but overlaps the number of parvalbumin-positive boutons. It is possible that boutons survive but stop expressing both parvalbumin and synaptotagmin-2. Synaptotagmin-1 can compensate for reduced expression of synaptotagmin-2 (Bouhours, Gjoni, Kochubey, & Schneggenburger, 2017). The most parsimonious scenario, however, is loss of some boutons and continued expression of parvalbumin and synaptotagmin-2 in remaining survivors.

In sclerotic hippocampi, reductions in parvalbumin-positive boutons were less severe than reductions in somata. Continued expression of parvalbumin-immunoreactivity in axon terminals during simultaneous loss of immunoreactivity in somata and dendrites occurs after cerebral ischemia (Johansen et al., 1990), in epileptic Mongolian gerbils (Nitsch et al., 1995; Scotti et al., 1997), in CA1 of epileptic pilocarpine-treated

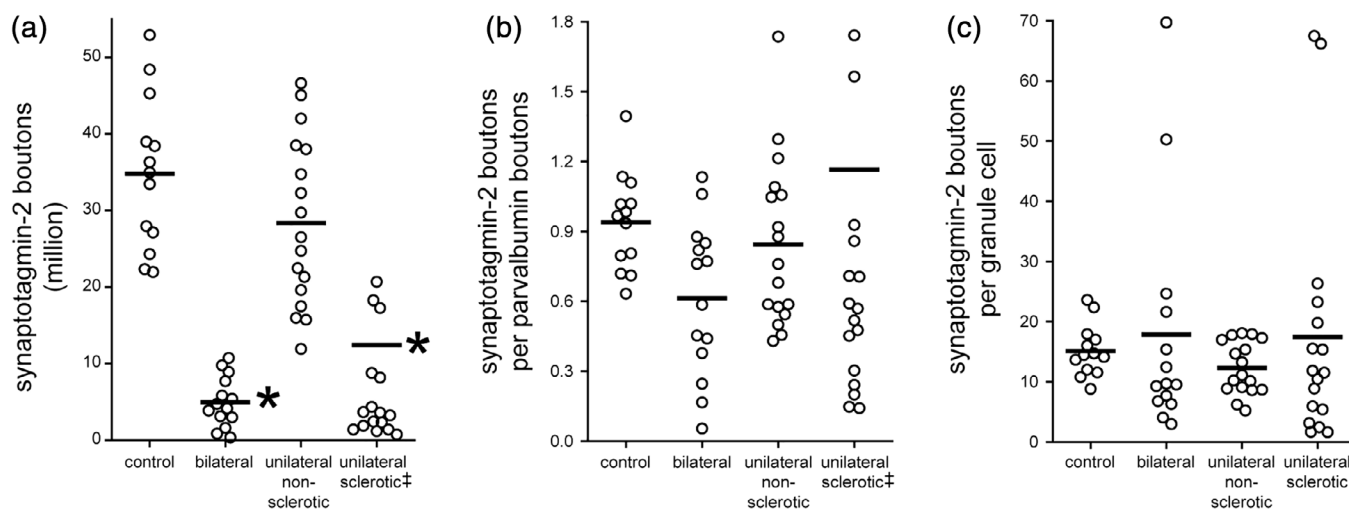


FIGURE 8 Number of synaptotagmin-2-immunoreactive boutons (panel a), synaptotagmin-2 boutons per parvalbumin bouton (panel b), and synaptotagmin-2 boutons per granule cell (panel c) in the dentate gyrus of control sea lions, sea lions with bilaterally sclerotic hippocampi, and sea lions with unilaterally sclerotic hippocampi (divided into nonsclerotic and sclerotic groups). Markers indicate values from individual sea lions. Bars indicate averages. Asterisks indicate significantly different from the control group, $p < .05$, Kruskal-Wallis ANOVA on ranks with Dunn's method. ‡Indicates groups in which one outlier value (>3.5 -times the standard deviation from the average) is higher than the y axis scale of the plot

rats (Dinocourt, Petanjek, Freund, Ben-Ari, & Esclapez, 2003), and in human TLE patients in which CA1 pyramidal cells are preserved (Wittner et al., 2005). Together, these findings suggest that the reduced number of parvalbumin-positive boutons in sclerotic hippocampi is attributable to genuine loss.

Sea lions with sclerotic hippocampi had a median of 16–26 parvalbumin-positive boutons per granule cell, which is similar to controls. This finding suggests the loss of parvalbumin-positive boutons is proportional to the loss of granule cells so that a balance remains in epileptic animals. It is unclear how this balance is achieved. It might simply be the loss of equal proportions of parvalbumin interneurons and granule cells. It might also involve axon remodeling. Parvalbumin interneuron microcircuitry changes dynamically under developmental (Chattopadhyaya et al., 2004, 2007; Donato, Rompani, & Caroni, 2013), experimental (Pieraut et al., 2014), and epileptic conditions (Christenson Wick, Leintz, Xamonthiene, Huang, & Krook-Magnuson, 2017).

The finding of proportional losses of parvalbumin-positive boutons and granule cells suggests parvalbumin interneuron-mediated inhibition of granule cells might be preserved. There are caveats to this conclusion, however. First, measuring bouton numbers is not the same as measuring synapses. Nevertheless, there is no significant difference in the average number of axosomatic synapses with granule cells per bouton in control and epileptic pilocarpine-treated rats (Buckmaster et al., 2016), so bouton numbers might be representative. Second, although average and median numbers of boutons per granule cell are not reduced in sclerotic hippocampi, some individual granule cells in sclerotic hippocampi might receive few if any parvalbumin-positive synapses. In sclerotic hippocampi, the meshwork of parvalbumin-positive axons and boutons often failed to extend to regions where granule cells were numerous. Similar patterns of PV bouton loss in the granule cell layer occur in human patients with TLE (Arellano et al., 2004; Sloviter et al., 1991; Wittner et al., 2001; Zhu et al., 1997) and in a minority of epileptic kainate-treated rats (Buckmaster & Dudek, 1997). Variability and patchiness in the innervation of excitatory neurons by parvalbumin-positive boutons has been proposed as an

epileptogenic mechanism (DeFelipe, 1999). However, in the dentate gyrus parvalbumin interneurons are only one of the sources of perisomatic inhibitory input to granule cells. Most axosomatic and axoaxonic symmetric synapses with granule cells are not parvalbumin-positive (Wittner et al., 2001), even in control tissue (Ribak et al., 1990). The type(s) of interneurons providing non-parvalbumin synaptic input to granule cell somata and axon initial segments remains unclear. Cholecystokinin-immunoreactive interneurons are not likely to be a major source, because their axons mostly target the inner molecular layer (Hefft & Jonas, 2005; Leranath & Frotscher, 1986). Regardless of the source, electron microscopic evidence suggests the number of inhibitory synapses with granule cell somata and axon initial segments are not significantly reduced in TLE (Thind et al., 2010; Wittner et al., 2001).

A final caveat is that regardless of whether there are proportional and balanced reductions in parvalbumin-positive synaptic boutons and granule cells, and even if other types of interneurons compensate for parvalbumin axon loss, anatomical preservation of synapses does not guarantee functionality. Basket cell-to-granule cell synaptic transmission is almost four-times more likely to fail in epileptic pilocarpine-treated rats compared to controls (Zhang & Buckmaster, 2009), and some parvalbumin-positive basket cells reduce their firing frequency seconds before spontaneous seizures begin (Toyoda, Fujita, Thamattoor, & Buckmaster, 2015). Therefore, parvalbumin interneurons might contribute to epilepsy through mechanisms other than anatomical loss of synaptic input to principal cells.

ACKNOWLEDGMENTS

We are grateful to Gina Rojas for help sectioning tissue and to staff of The Marine Mammal Center for assistance with animals and medical records. Animals were sampled under Marine Mammal Protection Act permit number 18786. Supported by NSF and NIH (NIEHS, NINDS, and OD).

DATA ACCESSIBILITY

Raw data supporting this article's findings are described in detail but have not been shared in a public repository. Please contact the corresponding author for further access to data.

ORCID

Paul S. Buckmaster  <https://orcid.org/0000-0003-1627-1799>

REFERENCES

- Amrein, I., Becker, A. S., Engler, S., Huang, S. H., Müller, J., Slomianka, L., & Oosthuizen, M. K. (2014). Adult neurogenesis and its anatomical context in the hippocampus of three mole-rat species. *Frontiers in Neuroanatomy*, 8, 39.
- Amrein, I., & Slomianka, L. (2010). A morphologically distinct granule cell type in the dentate gyrus of the red fox correlates with adult hippocampal neurogenesis. *Brain Research*, 1328, 12–24.
- André, V., Marescaux, C., Nehlig, A., & Fritschy, J. M. (2001). Alterations of hippocampal GABAergic system contribute to development of spontaneous seizures in the rat lithium-pilocarpine model of temporal lobe epilepsy. *Hippocampus*, 11, 452–468.
- Andrioli, A., Alonso-Nanclares, L., Arellano, J. I., & DeFelipe, J. (2007). Quantitative analysis of parvalbumin-immunoreactive cells in the human epileptic hippocampus. *Neuroscience*, 149, 131–143.
- Arellano, J. I., Muñoz, A., Ballesteros-Yáñez, I., Sola, R. G., & DeFelipe, J. (2004). Histopathology and reorganization of chandelier cells in the human epileptic sclerotic hippocampus. *Brain*, 127, 45–64.
- Austin, J. E., & Buckmaster, P. S. (2004). Recurrent excitation of granule cells with basal dendrites and low interneuron density and inhibitory postsynaptic current frequency in the dentate gyrus of macaque monkeys. *Journal of Comparative Neurology*, 476, 205–218.
- Babb, T. L., Pretorius, J. K., Kupfer, W. R., & Crandall, P. H. (1989). Glutamate decarboxylase-immunoreactive neurons are preserved in human epileptic hippocampus. *The Journal of Neuroscience*, 9, 2562–2574.
- Bahh, B. E., Lespinet, V., Lurton, D., Coussemacq, M., Le Gal La Salle, G., & Rougier, A. (1999). Correlations between granule cell dispersion, mossy fiber sprouting, and hippocampal cell loss in temporal lobe epilepsy. *Epilepsia*, 40, 1393–1401.
- Bazzett, T. J., Becker, J. B., Falik, R. C., & Albin, R. L. (1994). Chronic intrastriatal quinolinic acid produces reversible changes in perikaryal calbindin and parvalbumin immunoreactivity. *Neuroscience*, 60, 837–841.
- Blümcke, I., Pauli, E., Clusmann, H., Schramm, J., Becker, A., Elger, C., ... Hildebrandt, M. (2007). A new clinic-pathological classification system for mesial temporal sclerosis. *Acta Neuropathologica*, 113, 235–244.
- Bouhours, B., Gjoni, E., Kochubey, O., & Schneggenburger, R. (2017). Synaptotagmin2 (syt2) drives fast release redundantly with syt1 at the output synapses of parvalbumin-expressing inhibitory neurons. *The Journal of Neuroscience*, 37, 4604–4617.
- Braak, E., Strotkamp, B., & Braak, H. (1991). Parvalbumin-immunoreactive structures in the hippocampus of the human adult. *Cell and Tissue Research*, 264, 33–48.
- Buckmaster, P. S., Abrams, E., & Wen, X. (2017). Seizure frequency correlates with loss of dentate gyrus GABAergic neurons in a mouse model of temporal lobe epilepsy. *Journal of Comparative Neurology*, 525, 2592–2610.
- Buckmaster, P. S., & Dudek, F. E. (1997). Neuron loss, granule cell axon reorganization, and functional changes in the dentate gyrus of epileptic kainate-treated rats. *Journal of Comparative Neurology*, 385, 385–404.
- Buckmaster, P. S., & Lew, F. H. (2011). Rapamycin suppresses mossy fiber sprouting but not seizure frequency in a mouse model of temporal lobe epilepsy. *The Journal of Neuroscience*, 31, 2337–2347.
- Buckmaster, P. S., Wen, X., Toyoda, I., Gulland, F. M. D., & Van Bonn, W. (2014). Hippocampal neuropathology of domoic acid-induced epilepsy in California sea lions (*Zalophus californianus*). *Journal of Comparative Neurology*, 522, 1691–1706.
- Buckmaster, P. S., Yamawaki, R., & Thind, K. (2016). More docked vesicles and larger active zones at basket cell-to-granule cell synapses in a rat model of temporal lobe epilepsy. *The Journal of Neuroscience*, 36, 3295–3308.
- Celio, M. R. (1986). Parvalbumin in most gamma-aminobutyric acid-containing neurons of the rat cerebral cortex. *Science*, 231, 995–997.
- Chattopadhyaya, B., Di Cristo, G., Higashiyama, H., Knott, G. W., Kuhlman, S. J., Welker, E., & Huang, Z. J. (2004). Experience and activity-dependent maturation of perisomatic GABAergic innervation in primary visual cortex during a postnatal critical period. *The Journal of Neuroscience*, 24, 9598–9611.
- Chattopadhyaya, B., Di Cristo, G., Wu, C. Z., Knott, G., Kuhlman, S., Fu, Y., ... Huang, Z. J. (2007). GAD67-mediated GABA synthesis and signaling regulate inhibitory synaptic innervation in the visual cortex. *Neuron*, 54, 889–903.
- Christenson Wick, Z., Leintz, C. H., Xamonthiene, C., Huang, B. H., & Krook-Magnuson, E. (2017). Axonal sprouting in commissurally projecting parvalbumin-expressing interneurons. *Journal of Neuroscience Research*, 95, 2336–2344.
- Daniel, W. W. (1987). *Biostatistics: A foundation for analysis in the health sciences* (p. 222). New York, NY: John Wiley & Sons.
- DeFelipe, J. (1999). Chandelier cells and epilepsy. *Brain*, 122, 1807–1822.
- de Jong, G. I., Naber, P. A., Van der Zee, E. A., Thompson, L. T., Disterhoft, J. F., & Luiten, P. G. (1996). Age-related loss of calcium binding proteins in rabbit hippocampus. *Neurobiology of Aging*, 17, 459–465.
- de Lanerolle, N. C., Kim, J. H., Williamson, A., Spencer, S. S., Zaveri, H. P., Eid, T., & Spencer, D. D. (2003). A retrospective analysis of hippocampal pathology in human temporal lobe epilepsy: Evidence for distinctive patient subcategories. *Epilepsia*, 44, 677–687.
- Dinocourt, C., Petanjek, Z., Freund, T. F., Ben-Ari, Y., & Esclapez, M. (2003). Loss of interneurons innervating pyramidal cell dendrites and axon initial segments in the CA1 region of the hippocampus following pilocarpine-induced seizures. *Journal of Comparative Neurology*, 459, 407–425.
- Donato, F., Rompani, S. B., & Caroni, P. (2013). Parvalbumin-expressing basket-cell network plasticity induced by experience regulates adult learning. *Nature*, 504, 272–276.
- Elfving, B., Bonefeld, B. E., Rosenberg, R., & Wegener, G. (2008). Differential expression of synaptic vesicle proteins after repeated electroconvulsive seizures in rat frontal cortex and hippocampus. *Synapse*, 62, 662–670.
- Ferrer, I., Zujar, M. J., Admella, C., & Alcantara, S. (1992). Parvalbumin and calbindin immunoreactivity in the cerebral cortex of the hedgehog (*Eri-naceus europaeus*). *Journal of Anatomy*, 180, 165–174.
- Fox, M. A., & Sanes, J. R. (2007). Synaptotagmin I and II are present in distinct subsets of central synapses. *Journal of Comparative Neurology*, 503, 280–296.
- Franck, J. E., Pokorny, J., Kunkel, D. D., & Schwartzkroin, P. A. (1995). Physiologic and morphologic characteristics of granule cell circuitry in human epileptic hippocampus. *Epilepsia*, 36, 543–558.
- Fukuda, T., Aika, Y., Heizmann, C. W., & Kosaka, T. (1996). Dense GABAergic input on somata of parvalbumin-immunoreactive GABAergic neurons in the hippocampus of the mouse. *Neuroscience Research*, 26, 181–194.
- Gabriel, S., Njunting, M., Pomper, J. K., Merschhemke, M., Sanabria, E. R. G., Eilers, A., ... Lehmann, T. N. (2004). Stimulus and potassium-induced epileptiform activity in the human dentate gyrus from patients with and without hippocampal sclerosis. *The Journal of Neuroscience*, 24, 10416–10430.
- García-Junco-Clemente, P., Cantero, G., Gómez-Sánchez, L., Linares-Clemente, P., Martínez-López, J. A., Luján, R., & Fernández-Chacón, R. (2010). Cysteine string protein- α prevents activity-dependent degeneration in GABAergic synapses. *The Journal of Neuroscience*, 30, 7377–7391.
- Geppert, M., Archer, B. T., 3rd, & Südhof, T. C. (1991). Synaptotagmin II. A novel differentially distributed form of synaptotagmin. *The Journal of Biological Chemistry*, 266, 13548–13552.
- Goldstein, T., Mazet, J. A. K., Zabka, T. S., Langlois, G., Colegrove, K. M., Silver, M., ... Gulland, F. M. D. (2008). Novel symptomatology and changing epidemiology of domoic acid toxicosis in California sea lions (*Zalophus californianus*): An increasing risk to marine mammal health. *Proceedings of the Royal Society of London B: Biological Sciences*, 275, 267–276.
- Greig, D. J., Gulland, F. M. D., & Kreuder, C. (2005). A decade of live California sea lion (*Zalophus californianus*) strandings along the central California coast: Causes and trends, 1991–2000. *Aquatic Mammals*, 31, 11–22.

- Gulland, F. M. D., Haulena, M., Fauquier, D., Langlois, G., Lander, M. E., Zabka, T., & Duerr, R. (2002). Domoic acid toxicity in California sea lions (*Zalophus californianus*): Clinical signs, treatment and survival. *Veterinary Record*, *150*, 475–480.
- Hefft, S., & Jonas, P. (2005). Asynchronous GABA release generates long-lasting inhibition at a hippocampal interneuron-principal neuron synapse. *Nature Neuroscience*, *8*, 1319–1328.
- Hof, P. R., Rosenthal, R. E., & Fiskum, G. (1996). Distribution of neurofilament protein and calcium-binding proteins parvalbumin, calbindin, and calretinin in the canine hippocampus. *Journal of Chemical Neuroanatomy*, *11*, 1–12.
- Holm, I. E., Geneser, F. A., Zimmer, J., & Baimbridge, K. G. (1990). Immunocytochemical demonstration of the calcium-binding proteins calbindin-D 28k and parvalbumin in the subiculum, hippocampus and dentate area of the domestic pig. *Progress in Brain Research*, *83*, 85–97.
- Huusko, N., Römer, C., Ndode-Ekane, X. E., Lukasiuk, K., & Pitkänen, A. (2015). Loss of hippocampal interneurons and epileptogenesis: A comparison of two animal models of acquired epilepsy. *Brain Structure and Function*, *220*, 153–191.
- Jinno, S., & Kosaka, T. (2002). Patterns of expression of calcium binding proteins and neuronal nitric oxide synthase in different populations of hippocampal GABAergic neurons in mice. *Journal of Comparative Neurology*, *449*, 1–25.
- Johansen, F. F., Tønder, N., Zimmer, J., Baimbridge, K. G., & Diemer, N. H. (1990). Short-term changes of parvalbumin and calbindin immunoreactivity in the rat hippocampus following cerebral ischemia. *Neuroscience Letters*, *120*, 171–174.
- Keuer, J. I., Rochford, C. D., Witter, M. P., & Fuchs, E. (2003). A cytoarchitectonic study of the hippocampal formation of the tree shrew (*Tupaia belangeri*). *Journal of Chemical Neuroanatomy*, *26*, 1–15.
- Kim, J. E., Kwak, S. E., Kim, D. S., Won, M. H., Kwon, O. S., Choi, S. Y., & Kang, T. C. (2006). Reduced calcium binding protein immunoreactivity induced by electroconvulsive shock indicates neuronal hyperactivity, not neuronal death or deactivation. *Neuroscience*, *137*, 317–326.
- Kim, J. H., Guimaraes, P. O., Shen, M. Y., Masukawa, L. M., & Spencer, D. D. (1990). Hippocampal neuronal density in temporal lobe epilepsy with and without gliomas. *Acta Neuropathologica*, *80*, 41–45.
- Kobayashi, M., & Buckmaster, P. S. (2003). Reduced inhibition of dentate granule cells in a model of temporal lobe epilepsy. *The Journal of Neuroscience*, *23*, 2440–2452.
- Kosaka, T. (1996). Synapses in the granule cell layer of the rat dentate gyrus: Serial-sectioning study. *Experimental Brain Research*, *112*, 237–243.
- Kosaka, T., Katsumaru, H., Hama, K., Wu, J. Y., & Heizmann, C. W. (1987). GABAergic neurons containing the Ca²⁺-binding protein parvalbumin in the rat hippocampus and dentate gyrus. *Brain Research*, *419*, 119–130.
- Kraushaar, U., & Jonas, P. (2000). Efficacy and stability of quantal GABA release at a hippocampal interneuron-principal neuron synapse. *The Journal of Neuroscience*, *20*, 5594–5607.
- Leranth, C., & Frotscher, M. (1986). Synaptic connections of cholecystokinin-immunoreactive neurons and terminals in the rat fascia dentata: A combined light and electron microscopic study. *Journal of Comparative Neurology*, *254*, 51–64.
- Margerison, J. H., & Corsellis, J. A. (1966). Epilepsy and the temporal lobes. A clinical, electroencephalographic and neuropathological study of the brain in epilepsy, with particular reference to the temporal lobes. *Brain*, *89*, 499–530.
- Marquèze, B., Boudier, J. A., Mizuta, M., Inagaki, N., Seino, S., & Seagar, M. (1995). Cellular localization of synaptotagmin I, II, and III mRNAs in the central nervous system and pituitary and adrenal glands of the rat. *The Journal of Neuroscience*, *15*, 4906–4917.
- Masukawa, L. M., O'Connor, W. M., Lynott, J., Burdette, L. J., Uruno, K., McGonigle, P., & O'Connor, M. J. (1995). Longitudinal variation in cell density and mossy fiber reorganization in the dentate gyrus from temporal lobe epileptic patients. *Brain Research*, *678*, 65–75.
- Mathern, G. W., Babb, T. L., Leite, J. P., Pretorius, J. K., Yeoman, K. M., & Kuhlman, P. A. (1996). The pathogenic and progressive features of chronic human hippocampal epilepsy. *Epilepsy Research*, *26*, 151–161.
- Mathern, G. W., Babb, T. L., Pretorius, J. K., & Leite, J. P. (1995). Reactive synaptogenesis and neuron densities for neuropeptide Y, somatostatin, and glutamate decarboxylase immunoreactivity in the epileptogenic human fascia dentata. *The Journal of Neuroscience*, *15*, 3990–4004.
- Mathern, G. W., Kuhlman, P. A., Mendoza, D., & Pretorius, J. K. (1997). Human fascia dentata anatomy and hippocampal neuron densities differ depending on the epileptic syndrome and age at first seizure. *Journal of Neuropathology & Experimental Neurology*, *56*, 199–212.
- Mello, L. E. A. M., Cavalheiro, E. A., Tan, A. M., Kupfer, W. R., Pretorius, J. K., Babb, T. L., & Finch, D. M. (1993). Circuit mechanisms of seizures in the pilocarpine model of chronic epilepsy: Cell loss and mossy fiber sprouting. *Epilepsia*, *34*, 985–995.
- Mitchell, T. W., Buckmaster, P. S., Hoover, E. A., Whalen, L. R., & Dudek, F. E. (1999). Neuron loss and axon reorganization in the dentate gyrus of cats infected with the feline immunodeficiency virus. *Journal of Comparative Neurology*, *411*, 563–577.
- Montie, E. W., Wheeler, E., Pussini, N., Battey, T. W. K., Van Bonn, W., & Gulland, F. (2012). Magnetic resonance imaging reveals that brain atrophy is more severe in older California sea lions with domoic acid toxicosis. *Harmful Algae*, *20*, 19–29.
- Nacher, J., Palop, J. J., Ramirez, C., Molowny, A., & Lopez-Garcia, C. (2000). Early histological maturation in the hippocampus of the guinea pig. *Brain Behavior and Evolution*, *56*, 38–44.
- Nitsch, C., Scotti, A. L., & Nitsch, F. M. (1995). Distribution of parvalbumin-containing interneurons in the hippocampus of the gerbil—A qualitative and quantitative statistical analysis. *Journal of Chemical Neuroanatomy*, *9*, 135–147.
- Pang, Z. P., Melicoff, E., Padgett, D., Liu, Y., Teich, A. F., Dickey, B. F., ... Südhof, T. C. (2006). Synaptotagmin-2 is essential for survival and contributes to Ca²⁺ triggering of neurotransmitter release in central and neuromuscular synapses. *The Journal of Neuroscience*, *26*, 13493–13504.
- Pieraul, S., Gounko, N., Sando, R., 3rd, Dang, W., Rebboah, E., Panda, S., ... Maximov, A. (2014). Experience-dependent remodeling of basket cell networks in the dentate gyrus. *Neuron*, *84*, 107–122.
- Pitkänen, A., & Amaral, D. G. (1993). Distribution of parvalbumin-immunoreactive cells and fibers in the monkey temporal lobe: The hippocampal formation. *Journal of Comparative Neurology*, *331*, 37–74.
- Quesney, L. F. (1986). Clinical and EEG features of complex partial seizures of temporal lobe origin. *Epilepsia*, *27*(Supplement 2), S27–S45.
- Ribak, C. E., Nitsch, R., & Seress, L. (1990). Proportion of parvalbumin-positive basket cells in the GABAergic innervation of pyramidal and granule cells of the rat hippocampal formation. *Journal of Comparative Neurology*, *300*, 449–461.
- Sass, K. J., Spencer, D. D., Kim, J. H., Westerveld, M., Novelly, R. A., & Lencz, T. (1990). Verbal memory impairment correlates with hippocampal pyramidal cell density. *Neurology*, *40*, 1694–1697.
- Scholín, C. A., Gulland, F., Boucette, G. J., Benson, S., Busman, M., Chavez, F. P., ... Van Dolah, F. M. (2000). Mortality of sea lions along the central California coast linked to a toxic diatom bloom. *Nature*, *304*, 80–84.
- Scotti, A. L., Bollag, O., Kalt, G., & Nitsch, C. (1997). Loss of perikaryal parvalbumin immunoreactivity from surviving GABAergic neurons in the CA1 field of epileptic gerbils. *Hippocampus*, *7*, 524–535.
- Seress, L., Gulyás, A. I., Ferrer, I., Tunon, T., Soriano, E., & Freund, T. F. (1993). Distribution, morphological features, and synaptic connections of parvalbumin- and calbindin D28k-immunoreactive neurons in the human hippocampal formation. *Journal of Comparative Neurology*, *337*, 208–230.
- Seress, L., Gulyás, A. I., & Freund, T. F. (1991). Parvalbumin- and calbindin D28k-immunoreactive neurons in the hippocampal formation of the macaque monkey. *Journal of Comparative Neurology*, *313*, 162–177.
- Seress, L., & Ribak, C. E. (1992). Ultrastructural features of primate granule cell bodies show important differences from those of rats: Axosomatic synapses, somatic spines and infolded nuclei. *Brain Research*, *569*, 353–357.
- Seto-Ohshima, A., Aoki, E., Semba, R., Emson, P. C., & Heizmann, C. W. (1990). Appearance of parvalbumin-specific immunoreactivity in the cerebral cortex and hippocampus of the developing rat and gerbil brain. *Histochemistry*, *94*, 579–589.
- Shao, L. R., & Dudek, F. E. (2005). Changes in mIPSCs and sIPSCs after kainate treatment: Evidence for loss of inhibitory input to dentate granule cells and possible compensatory responses. *Journal of Neurophysiology*, *94*, 952–960.

- Sik, A., Penttonen, M., Ylinen, A., & Buzsáki, G. (1995). Hippocampal CA1 interneurons: An in vivo intracellular labeling study. *The Journal of Neuroscience*, *15*, 6651–6665.
- Silvagni, P. A., Lowenstine, L. J., Spraker, T., Lipscomb, T. P., & Gulland, F. M. (2005). Pathology of domoic acid toxicity in California sea lions (*Zalophus californianus*). *Veterinary Pathology*, *42*, 184–191.
- Slomianka, L., Drenth, T., Cavegn, N., Menges, D., Lazic, S. E., ... Amrein, I. (2013). The hippocampus of the eastern rock sengi: Cytoarchitecture, markers of neuronal function, principal cell numbers, and adult neurogenesis. *Frontiers in Neuroanatomy*, *7*, 34.
- Sloviter, R. S., Sollas, A. L., Barbaro, N. M., & Laxer, K. D. (1991). Calcium-binding protein (calbindin-D28K) and parvalbumin immunocytochemistry in the normal and epileptic human hippocampus. *Journal of Comparative Neurology*, *308*, 381–396.
- Soltész, I., Smetters, D. K., & Mody, I. (1995). Tonic inhibition originates from synapses close to the soma. *Neuron*, *14*, 1273–1283.
- Sommeijer, J., & Levitt, C. N. (2012). Synaptotagmin-2 is a reliable marker for parvalbumin positive inhibitory boutons in the mouse visual cortex. *PLoS One*, *7*, e35323.
- Spanedda, F., Cendes, F., & Gotman, J. (1997). Relations between EEG seizure morphology, interhemispheric spread, and mesial temporal atrophy in bitemporal epilepsy. *Epilepsia*, *38*, 1300–1314.
- Spencer, S. S., Williamson, P. D., Spencer, D. D., & Mattson, R. H. (1987). Human hippocampal seizure spread studied by depth and subdural recording: The hippocampal commissure. *Epilepsia*, *28*, 479–489.
- Sperling, M. R., & O'Connor, M. J. (1989). Comparison of depth and subdural electrodes in recording temporal lobe seizures. *Neurology*, *39*, 1497–1504.
- Südhof, T. C. (2013). Neurotransmitter release: The last millisecond in the life of a synaptic vesicle. *Neuron*, *80*, 675–690.
- Sun, C., Mtchedlishvili, Z., Bertram, E. H., Erisir, A., & Kapur, J. (2007). Selective loss of dentate hilar interneurons contributes to reduced synaptic inhibition of granule cells in an electrical stimulation-based model of temporal lobe epilepsy. *Journal of Comparative Neurology*, *500*, 876–893.
- Thind, K. K., Yamawaki, R., Phanwar, I., Zhang, G., Wen, X., & Buckmaster, P. S. (2010). Initial loss but later excess of GABAergic synapses with dentate granule cells in a rat model of temporal lobe epilepsy. *Journal of Comparative Neurology*, *518*, 647–667.
- Thomas, K., Harvey, J. T., Goldstein, T., Barakos, J., & Gulland, F. (2010). Movement, dive behavior, and survival of California sea lions (*Zalophus californianus*) posttreatment for domoic acid toxicosis. *Marine Mammal Science*, *26*, 36–52.
- Tortosa, A., & Ferrer, I. (1993). Parvalbumin immunoreactivity in the hippocampus of the gerbil after transient forebrain ischaemia: A qualitative sequential study. *Neuroscience*, *55*, 33–43.
- Toyoda, I., Fujita, S., Thamattoor, A. K., & Buckmaster, P. S. (2015). Unit activity of hippocampal interneurons before spontaneous seizures in an animal model of temporal lobe epilepsy. *The Journal of Neuroscience*, *35*, 6600–6618.
- Trevarrow, B., Marks, D. L., & Kimmel, C. B. (1990). Organization of hind-brain segments in the zebrafish embryo. *Neuron*, *4*, 669–679.
- van Vliet, E. A., Aronica, E., Tolner, E. A., Lopes da Silva, F. H., & Gorter, J. A. (2004). Progression of temporal lobe epilepsy in the rat is associated with immunocytochemical changes in inhibitory interneurons in specific regions of the hippocampal formation. *Experimental Neurology*, *187*, 367–379.
- West, M. J., Slomianka, L., & Gundersen, H. J. (1991). Unbiased stereological estimation of the total number of neurons in the subdivisions of the rat hippocampus using the optical fractionator. *The Anatomical Record*, *231*, 482–497.
- Williamson, A., Patrylo, P. R., & Spencer, D. D. (1999). Decrease in inhibition in dentate granule cells from patients with temporal lobe epilepsy. *Annals of Neurology*, *45*, 92–99.
- Williamson, A., Spencer, S. S., & Spencer, D. D. (1995). Depth electrode studies and intracellular dentate granule cell recordings in temporal lobe epilepsy. *Annals of Neurology*, *38*, 778–787.
- Wittner, L., Eross, L., Czirják, S., Halász, P., Freund, T. F., & Maglóczy, Z. (2005). Surviving CA1 pyramidal cells receive intact perisomatic inhibitory input in the human epileptic hippocampus. *Brain*, *128*, 138–152.
- Wittner, L., Maglóczy, Z., Borhegyi, Z., Halász, P., Tóth, S., Eröss, L., ... Freund, T. F. (2001). Preservation of perisomatic inhibitory input of granule cells in the epileptic human dentate gyrus. *Neuroscience*, *108*, 587–600.
- Yamawaki, R., Thind, K., & Buckmaster, P. S. (2015). Blockade of excitatory synaptogenesis with proximal dendrites of dentate granule cells following rapamycin treatment in a mouse model of temporal lobe epilepsy. *Journal of Comparative Neurology*, *523*, 281–297.
- Zhang, W., & Buckmaster, P. S. (2009). Dysfunction of the dentate basket cell circuit in a rat model of temporal lobe epilepsy. *The Journal of Neuroscience*, *29*, 7846–7856.
- Zhu, Z. Q., Armstrong, D. L., Hamilton, W. J., & Grossman, R. G. (1997). Disproportionate loss of CA4 parvalbumin-immunoreactive interneurons in patients with Ammon's horn sclerosis. *Journal of Neuropathology & Experimental Neurology*, *56*, 988–998.

How to cite this article: Cameron S, Lopez A, Glabman R, et al. Proportional loss of parvalbumin-immunoreactive synaptic boutons and granule cells from the hippocampus of sea lions with temporal lobe epilepsy. *J Comp Neurol*. 2019;527: 2341–2355. <https://doi.org/10.1002/cne.24680>